


RESEARCH ARTICLE

Open Access



A novel PSMA-targeting tracer with highly negatively charged linker demonstrates decreased salivary gland uptake in mice compared to [⁶⁸Ga]Ga-PSMA-11

Steve S. Huang^{1,2*} , Frank P. DiFilippo¹, Daniel J. Lindner¹ and Warren D. Heston¹

*Correspondence:
huang.steve2@mayo.edu

¹ Cleveland Clinic, 9500 Euclid
Ave, Cleveland, OH 44195, USA

² Department of Radiology,
Mayo Clinic, 13400 E. Shea Blvd.,
Scottsdale, AZ 85259, USA

Abstract

Background: The current generation of radiolabeled PSMA-targeting therapeutic agents is limited by prominent salivary gland binding, which results in dose-limiting xerostomia from radiation exposure. JB-1498 is a urea-based small molecule with a highly negatively charged linker targeting prostate specific membrane antigen (PSMA). Prior work on a similar tracer with the same negatively charged linker demonstrated low normal organ/soft tissue background uptake compared to [⁶⁸Ga]Ga-PSMA-11. The purpose of this study was to investigate if [⁶⁸Ga]Ga-JB-1498 had reduced salivary gland uptake in mice compared to [⁶⁸Ga]Ga-PSMA-11.

Results: JB-1498 demonstrated high affinity for PSMA binding and tumor uptake in a murine tumor model. In an initial biodistribution study with low molar activity, [⁶⁸Ga]Ga-JB-1498 demonstrated salivary gland uptake of $0.13 \pm 0.01\% \text{ID/g}$. In a second biodistribution study in non-tumor-bearing mice with high molar activity, [⁶⁸Ga]Ga-JB1498 demonstrated salivary gland uptake of $0.39 \pm 0.24\% \text{ID/g}$ and kidney activity of $10.12 \pm 1.73\% \text{ID/g}$ at one hour post IV injection. This salivary gland uptake is significantly less than the published uptake of [⁶⁸Ga]Ga-PSMA-11. Micro-PET visually confirmed the findings of the biodistribution studies. Dynamic micro-PET imaging demonstrated gradually decreasing [⁶⁸Ga]Ga-JB1498 activity in salivary glands and kidneys, compared to gradually increasing [⁶⁸Ga]Ga-PSMA-11 activity in these two organs during the first hour.

Conclusion: Biodistribution and micro-PET imaging of [⁶⁸Ga]Ga-JB-1498 demonstrate significantly decreased salivary gland uptake and different pharmacokinetic behavior in kidneys and salivary glands in mice compared to [⁶⁸Ga]Ga-PSMA-11. Our findings suggest that constructing a PSMA-targeting molecule with a highly negatively charged linker is a promising strategy to reduce salivary gland uptake of GCP-II/PSMA ligands in theranostic applications.

Keywords: PSMA, GCP-II, Prostate cancer, Salivary gland toxicity

Background

Prostate cancer is the most frequent non-cutaneous cancer and the second most frequent cause of cancer deaths in adult men (Siegel et al. 2023). Metastatic castration-resistant prostate cancer has a poor prognosis, with an estimated 34,700 prostate cancer deaths in the United States in 2023.

Glutamate carboxypeptidase II (GCP-II), or prostate specific membrane antigen (PSMA), is highly expressed in prostate cancers (Bostwick et al. 1998). Positron emission tomography with PSMA-targeting tracers that evolved over the last 20 years has proven to be the most accurate diagnostic modality for detecting metastatic prostate cancer non-invasively (Hope et al. 2019). In addition to PET imaging, therapeutic trials targeting PSMA have been conducted. The landmark VISION trial with [¹⁷⁷Lu]Lu-PSMA-617 for metastatic castration-resistant prostate cancer demonstrated prolonged survival compared to standard of care (Sartor et al. 2021). The VISION trial led to the FDA approval of [¹⁷⁷Lu]Lu-PSMA-617 for patients with PSMA-expressing metastatic prostate cancer. Despite the impressive results, the current 7.4 GBq (200 mCi) [¹⁷⁷Lu]Lu-PSMA-617 regimen is a compromise of efficacy and side effects with 9% complete response and 42% partial response. Replacing ¹⁷⁷Lu with an alpha emitter (i.e. [²²⁵Ac]Ac-PSMA-617) can further improve the response (Feuerecker et al. 2021). In fact, one of the first human trials of [²²⁵Ac]Ac-PSMA-617 demonstrated an impressive response where the PSA value of a patient with metastatic prostate cancer was reduced from 2,923 ng/mL to less than 0.1 ng/mL after 4 cycles of therapy with [²²⁵Ac]Ac-PSMA-617 (Kratochwil et al. 2016). [²²⁵Ac]Ac-PSMA-I&T and [¹⁷⁷Lu]Lu-PSMA-I&T, now emerging from the clinical trial pipeline toward approval, demonstrate similar biodistribution and comparable efficacy/toxicity profile as PSMA-617 based agents (Zacherl et al. 2021; Schuchardt et al. 2022).

A consistent limitation of the current generation of ²²⁵Ac-PSMA therapeutic agents is the dose limiting xerostomia from salivary gland and lacrimal gland radiation exposure (Kratochwil et al. 2017; Taieb et al. 2018). A GCP-II targeting ligand with reduced salivary gland uptake has the potential to decrease salivary gland toxicity and increase therapeutic window of PSMA targeting radiotherapy.

[²²⁵Ac]Ac-PSMA-617/[¹⁷⁷Lu]Lu-PSMA-617 tandem therapy with reduced dose ²²⁵Ac-PSMA therapeutic agents has been tried in an effort to decrease salivary gland toxicity (Khreish et al. 2020). Many strategies have been employed to try to reduce salivary gland uptake of PSMA-targeting agents. Methods include external cooling (Kalmthout et al. 2018), co-administration of PSMA inhibitors using PMPA (Kratochwil et al. 2015) and unlabeled PSMA-11 (Kalidindi et al. 2021), ductal injection of DCFPyL (Roy et al. 2021), botulinum toxin (Baum et al. 2018), muscarinic inhibition (Mohan et al. 2021), monosodium glutamate administration (Rousseau et al. 2018), and vitamin C administration (Yu et al. 2022). While the above-listed efforts focus on suppressing the salivary gland uptake of PSMA-targeting ligands, there is evidence emerging that salivary gland uptake of PSMA targeting ligands can be greatly reduced by manipulating the molecular framework. Kuo et al. demonstrated that replacing the glutamate sidechain of the Lys-urea-Glu pharmacophore at the catalytic site can lead to significant reduction of salivary gland uptake (Kuo et al. 2022).

Herein, we present preliminary data in mice that constructing a PSMA-targeting molecule with a highly negatively charged linker without altering the glutamate pharmacophore at the catalytic site is another potential strategy to reduce salivary gland uptake.

Materials and methods

All chemicals were reagent grade as detailed in the Additional file 1. JB-1498 (Fig. 1) was derived from structure “5” of prior work by Huang et al. (Additional file 1: Fig. 7) by replacing the Bn-NOTA chelate with DOTA (Huang et al. 2014). JB-1498 was synthesized using Fmoc-based solid phase peptide synthesis using Rink amid resin as the solid support and purified by HPLC as detailed in the Additional file 1.

Binding affinity of JB-1498 toward GCP-II was determined using fluorescent enzymatic inhibition assay (Kozikowski et al. 2004) as detailed in the Additional file 1.

In general, radiolabeling can be achieved by heating JB1498 in aqueous sodium acetate solution at pH 4–5 at 95 °C or above for 7–10 min. Radiolabeling reactions were optimized over time. Small variations in conditions in the reactions presented below were results of iterative changes. Please refer to Additional file 1 for HPLC traces of the initial radiolabeling trial (Additional file 1: Fig. 2 and Fig. 3).

Radiolabeling of JB-1498 for the initial biodistribution study was performed using $[^{68}\text{Ga}]\text{GaCl}_3$ from a spent $^{68}\text{Ge}/^{68}\text{Ga}$ generator from Isotopen Technologies Garching (Garching, Germany, currently ITM). JB-1498 with $[^{68}\text{Ga}]\text{GaCl}_3$ was heated in aqueous sodium acetate buffer at pH 4–5 and 97 °C for 7 min. The reaction product was HPLC-purified for the biodistribution study as detailed in the Additional file 1. The molar activity of the purified product was less than 7.4 GBq/ μmol (200 Ci/mmol) at the conclusion of synthesis.

For the high molar activity biodistribution and imaging study, a fresh 1.85 GBq (50mCi) GalliaPharm Gallium-68 generator from Eckert & Ziegler (Berlin, Germany) was used. Radiolabeling of JB-1498 with $[^{68}\text{Ga}]\text{GaCl}_3$ was performed in aqueous sodium acetate buffer at pH 4–5 and 98 °C for 10 min. The reaction product was diluted with water, loaded onto an Oasis HLB cartridge, washed with water, and eluted with 2:1 PBS:EtOH as detailed in the Additional file 1. The fractions with highest radioactivity were diluted with saline for injection in mice. Please refer to Additional file 1: Figs. 4 and Fig. 5 for HPLC traces of the products prior to and after solid phase extraction. The molar activity of the purified product was estimated to be 59 GBq/ μmol (1600 Ci/mmol) at the time of first injection. $[^{68}\text{Ga}]\text{Ga}$ -PSMA-11 was produced concurrently by incubating $[^{68}\text{Ga}]\text{GaCl}_3$ and PSMA-11 precursor in sodium acetate buffer at pH 4–5 at room

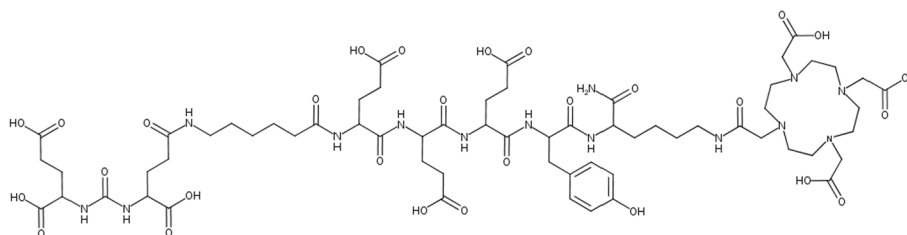


Fig. 1 Structure of JB-1498, a PSMA/GCP-II targeting molecule with a highly negatively charged linker between the urea and the DOTA chelate

temperature for 10 min. Please refer to Additional file 1: Fig. 6 for HPLC trace of the product. The molar activity of the product was estimated to be 48 GBq/ μ mol (1300 Ci/mmol) at the time of first injection.

For the initial biodistribution study in tumor bearing mice, 3 male 10 week-old NSG mice (NOD.Cg-Prkdc^{scid}Il2rg^{tm1Wjl}/SzJ) were inoculated subcutaneously with 4 million cells of PC3-PIP PSMA-expressing cell line. Mice were housed in a specific pathogen free, temperature- and humidity-controlled environment, in standard micro-isolator top cages with ad libitum access to chow. Biodistribution studies were conducted when the long axis of the tumor exceeded 1 cm. Each mouse was injected with 100 μ L of the [⁶⁸Ga]Ga-JB-1498 solution under isoflurane anesthesia via retro-orbital injection in the right eye and euthanized 1 h after injection. Major organs (including the left salivary glands) were dissected for radioactivity quantification. The dose injected was 0.74 ± 0.27 MBq.

For the high molar activity biodistribution study aimed at maximizing salivary gland uptake, 3 male NSG mice without tumor were injected with 100 μ L of the [⁶⁸Ga]Ga-JB-1498 solution under anesthesia via retro-orbital injection per the above-described protocol. The dose injected was 1.31 ± 0.26 MBq.

For the micro-PET imaging study, high molar activity [⁶⁸Ga]Ga-JB-1498 and [⁶⁸Ga]Ga-PSMA-11 were administered to non-tumor bearing NSG mice via tail vein injection. The dose injected was 5.3 MBq of [⁶⁸Ga]Ga-PSMA-11 and 4.4 MBq of [⁶⁸Ga]Ga-JB-1498. Imaging was performed on a nanoScan PET/CT instrument (Mediso USA, Arlington, Virginia). List mode PET acquisition was performed for 45 min starting 25 min post-injection. CT was performed for PET attenuation correction and anatomic localization.

Results

By mass spectrometry, the singly charged form of the purified JB-1498 sample had a mass of 1497.66 Da, matching the expected molecular structure of JB-1498 (Fig. 1). Using fluorescent enzymatic assay, EC₅₀ of JB-1498 was estimated to be 287 ± 64 pM (Additional file 1: Fig. 1). This places the upper limit of K_i of JB1498 to PSMA = 300 pM (K_i is lower than 300 pM).

The initial biodistribution study performed using an aged ITG Ga-68 generator (with estimated molar activity less than 7.4 GBq/ μ mol or 200 Ci/mmol) demonstrated tumor uptake of $12.09 \pm 1.28\%$, salivary gland uptake of $0.13 \pm 0.01\%$ and liver uptake of $0.20 \pm 0.09\%$ (Additional file 1: Table 1). We conducted an additional biodistribution study in non-tumor-bearing-mice with high molar activity [⁶⁸Ga]Ga-JB1498 at one hour post IV tracer injection and demonstrated salivary gland activity of $0.39 \pm 0.24\%$ ID/g and kidney activity of $10.12 \pm 1.73\%$ ID/g (Additional file 1: Table 2). The uptake values in these two organs are much lower than the [⁶⁸Ga]Ga-PSMA-11 salivary gland uptake of $10.00 \pm 2.52\%$ ID/g and kidney uptake of $182.0 \pm 33.5\%$ ID/g at one hour after injection as published by Rousseau et al. (2018) (Additional file 1: Table 3). Please note that the strain of mouse in this study is identical to that used by Rousseau et al. The molar activity and injected doses are all within the range specified by Rousseau et al.

Micro-PET images of mice at 1 h post-injection of [⁶⁸Ga]Ga-JB-1498 and [⁶⁸Ga]Ga-PSMA-11 visually confirmed much lower salivary gland and kidney uptake with [⁶⁸Ga]Ga-JB-1498 compared to [⁶⁸Ga]Ga-PSMA-11 (Fig. 2).

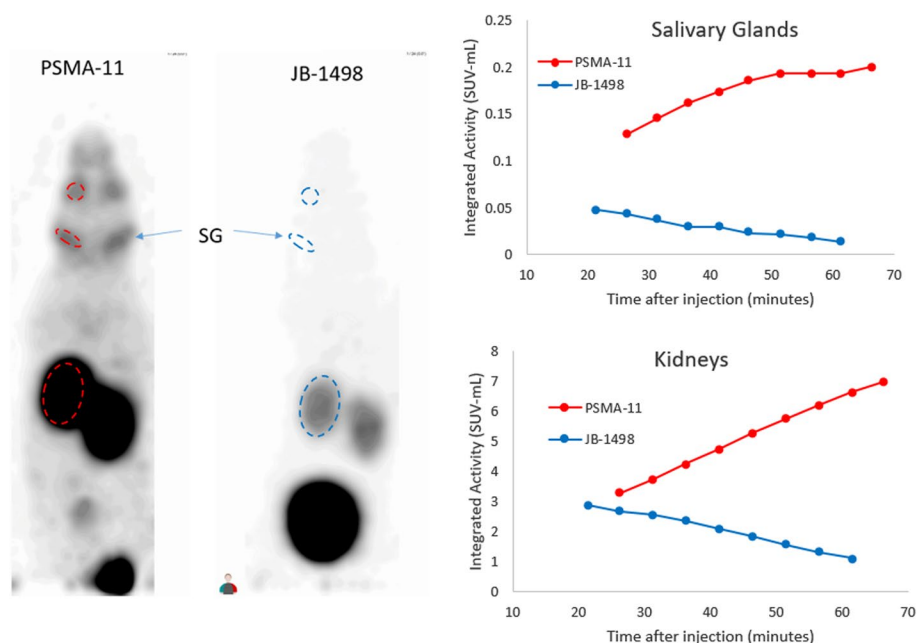


Fig. 2 Left panel: [^{68}Ga]Ga-PSMA-11 and [^{68}Ga]Ga-JB-1498 head-to-head comparison micro-PET images at 1 h post injection, with same SUV grayscale. There is very little salivary gland (SG) and background activity in the mouse injected with [^{68}Ga]Ga-JB-1498 compared to [^{68}Ga]Ga-PSMA-11. Most of the injected [^{68}Ga]Ga-JB-1498 is in the urinary bladder due to rapid tracer excretion via the kidneys. Right Panel: representative time-activity curve of [^{68}Ga]Ga-PSMA-11 and [^{68}Ga]Ga-JB-1498 in salivary glands (combined parotid and submandibular glands) and kidneys during the first hour of micro-PET imaging. The diverging time activity curve reflects active salivary gland and renal cortical uptake of [^{68}Ga]Ga-PSMA-11 and lack of specific uptake of [^{68}Ga]Ga-JB-1498 in these two organs

Discussion

The need to reduce salivary gland toxicity associated with current GCP-II catalytic site targeted treatment is widely recognized. However, the ability to systematically test a GCP-II targeting compound's propensity for salivary gland uptake was not available when the issue was first recognized. Rousseau et al. first demonstrated a testable experimental system where salivary gland uptake was consistently reproduced in mice with [^{68}Ga]Ga-PSMA-11 at 82.6 ± 44.3 GBq/ μmol (2230 ± 1200 Ci/mmol) molar activity (Rousseau et al. 2018). Roy et al. validated mice as a testable experimental model for salivary gland uptake using ^{18}F -DCFPyL (molar activity of 44–96 GBq/ μmol or 1200–2600 Ci/mmol) (Roy et al. 2020).

We had designed GCP-II inhibitors with highly negatively charged linkers with three glutamates a decade ago (Huang et al. 2014; Laydner et al. 2013). A ^{18}F -AIF labeled variant of the negatively charged linkers demonstrated rapid renal parenchymal wash-out and generally low normal organ activity at one hour post injection compared to other tracers published at the time. Initial PET imaging at the time demonstrated no significant salivary gland uptake. We were intrigued by the findings and subsequently constructed a variant of the molecule by replacing the Bn-NOTA chelate with DOTA (JB-1498). Replacement of the thiourea with the amide bond for chelator conjugation was necessary due to the propensity for radiolysis of the radiolabeled compound at high molar activity (see Additional file 1: Figs. 8–11).

In the initial biodistribution experiment, [^{68}Ga]Ga-JB-1498 demonstrated near background activity in salivary glands in mice and much lower renal cortical activity compared to published biodistribution data for [^{68}Ga]Ga-PSMA-11 (Rousseau et al. 2018). This correlates well with the imaging and biodistribution study of the ^{18}F -AIF labeled variant of the molecule with a negatively charged linker (Huang et al. 2014). However, our initial biodistribution studies were not in the range of molar activity reported in literature where [^{68}Ga]Ga-PSMA-11 demonstrated significant salivary gland uptake. Molar activity of PSMA-targeting ligands has been shown to affect organ uptake in mouse biodistribution studies (Khreish et al. 2020; Wurzer et al. 2018). To allow for maximal salivary gland uptake of ^{68}Ga -JB-1498 in high molar activity, we conducted a biodistribution study in non-tumor bearing mice using the eluate of a new ^{68}Ga generator for radiolabeling of JB-1498. A fresh ^{68}Ga generator allowed us to produce high molar activity [^{68}Ga]Ga-JB-1498 specified by Rousseau et al. (2018), Roy et al. (2020). We used non-tumor-bearing mice for the high-specific-activity experiment to maximize normal organ uptake. Salivary gland uptake of [^{68}Ga]Ga-JB1498 at high molar activity increased slightly compared to the lower molar activity experiment, indicating there is some effect of competition by the cold compound in mice. Nevertheless, [^{68}Ga]Ga-JB-1498 exhibited much lower salivary gland and renal cortical uptake compared to [^{68}Ga]Ga-PSMA-11. Dynamic micro-PET imaging demonstrates drastic differences in pharmacodynamic behavior in the salivary gland and renal cortex between [^{68}Ga]Ga-JB-1498 and [^{68}Ga]Ga-PSMA-11.

The cause of salivary gland uptake has been debated in the literature (Lucaroni et al. 2023; Lee et al. 2023; Huang et al. 2023; Bassi et al. 2023). The mechanisms of salivary gland uptake and, for that matter, the mechanisms of reduction of salivary gland uptake are still unclear. At first glance, our work seems to suggest that salivary gland uptake of PSMA-11 is unrelated to PSMA. However, one should be cautious that findings in mice may not translate to humans and further studies are needed. Our findings indicate that there may be several methods of structural modification targeting different regions that have the potential to alter salivary gland and renal cortex tracer uptake of PSMA-targeting small molecules. One is the replacement of the glutamate sidechain of the Lys-urea-Glu pharmacophore demonstrated by Kuo et al. (2022). Of note, the glutamate pharmacophore altered by Kuo et al. has been “conserved” in all urea-based high affinity PSMA targeting agents since the publication of its synthetic method by Kozikowski et al. (2001). Optimization of halogen positioning within the molecular framework of the inhibitor without altering the glutamate pharmacophore has also led to reduction of salivary gland uptake in mice (Mease et al. 2022). A potential new target of structural modification without altering the glutamate pharmacophore is the overall charge in the linker region as illustrated herein.

There is much yet to learn about tracer interaction with GCP-II/PSMA or possibly other GCP-like molecules. We have high hopes that future studies will lead to significant reduction of salivary/lacrimal gland toxicity, and profoundly widen the therapeutic window of PSMA-targeted therapies.

Supplementary Information

The online version contains supplementary material available at <https://doi.org/10.1186/s41181-024-00237-3>.

Additional file 1. Supplemental Data.

Acknowledgements

We would like to acknowledge Thomas Hattier and other present and past staff at the Cleveland Innovations, including Jason Ospina for invaluable administrative support. Tumor model and animal imaging procedures were performed by the Cleveland Clinic's Animal Tumor Core and Small Animal Imaging Core, directed by Daniel Lindner, MD, PhD, and Caroline Androjna, DEng, respectively. Studies were supported in part by the Case Comprehensive Cancer Center Athymic Animal and Preclinical Therapeutics Shared Resource and NCI core Grant 5 P30 CA043703-32. The nanoScan PET/CT instrument was purchased via an NIH shared instrumentation Grant S10-OD025042.LC-MS: Mass spectrometry performed by the Proteomics and Metabolomics Core is directed by Belinda Willard, PhD. The Fusion Lumos instrument was purchased via an NIH shared instrument Grant, S10 OD023436. The timsTof Pro2 instrument was purchased via an NIH shared instrument Grant, S10 OD030398.

Author contributions

All authors were involved in conceptual design of the experiment and manuscript editing. SSH performed synthesis, purification and radiolabeling. SSH performed fluorescent enzymatic inhibition assay with DJL assistance. FPD performed animal imaging and image data analysis. DJL prepared the mouse tumor model. SSH and DJL performed biodistribution study. All authors read and approved the final manuscript.

Funding

Ohio Department of Development, Ohio Third Frontier TVSF Grant TECH 2015-0779, 2017-0053.

Availability of data and materials

Detailed methods, binding and biodistribution data are included in the Additional file 1. Additional data will be made available on reasonable request.

Declarations

Ethics approval

Animal studies: Animal experiments using mice were performed in accordance with recommendations in Guide for the Care and Use of Laboratory Animals of the National Institutes of Health, and conducted under protocol number CCF IACUC2464 approved by Cleveland Clinic Institutional Animal Care and Use Committee.

Consent for publication

Not applicable.

Competing Interest

Steve Huang: the author filed a patent application with Cleveland Clinic Innovations regarding JB-1498. There is otherwise no conflict of interest. Frank DiFilippo: no conflict of interest. Daniel Lindner: no conflict of interest. Warren Heston: no conflict to interest.

Received: 22 November 2023 Accepted: 18 January 2024

Published online: 30 January 2024

References

- Bassi G, Cazzamalli S, Oehler S, Lucaroni L, Georgiev T, Favalli N, et al. Response to: GCP III is not the "off-target" for urea-based PSMA-ligands. *Eur J Nucl Med Mol Imaging*. 2023;50:2947–9. <https://doi.org/10.1007/s00259-023-06302-4>.
- Baum RP, Langbein T, Singh A, Shahinfar M, Schuchardt C, Volk GF, et al. Injection of botulinum toxin for preventing salivary gland toxicity after PSMA radioligand therapy: an empirical proof of a promising concept. *Nucl Med Mol Imaging*. 2018;52:80–1. <https://doi.org/10.1007/s13139-017-0508-3>.
- Bostwick DG, Pacelli A, Blute M, Roche P, Murphy GP. Prostate specific membrane antigen expression in prostatic intraepithelial neoplasia and adenocarcinoma: a study of 184 cases. *Cancer*. 1998;82:2256–61. [https://doi.org/10.1002/\(sici\)1097-0142\(19980601\)82:11%3c2256::aid-cnrc22%3e3.0.co;2-s](https://doi.org/10.1002/(sici)1097-0142(19980601)82:11%3c2256::aid-cnrc22%3e3.0.co;2-s).
- Feuerrecker B, Tauber R, Knorr K, Heck M, Beheshti A, Seidl C, et al. Activity and adverse events of actinium-225-PSMA-617 in advanced metastatic castration-resistant prostate cancer after failure of lutetium-177-PSMA. *Eur Urol*. 2021;79:343–50. <https://doi.org/10.1016/j.eururo.2020.11.013>.
- Hope TA, Goodman JZ, Allen IE, Calais J, Fendler WP, Carroll PR. Metaanalysis of (68)Ga-PSMA-11 PET accuracy for the detection of prostate cancer validated by histopathology. *J Nucl Med*. 2019;60:786–93. <https://doi.org/10.2967/jnumed.118.219501>.
- Huang SS, Wang X, Zhang Y, Doke A, DiFilippo FP, Heston WD. Improving the biodistribution of PSMA-targeting tracers with a highly negatively charged linker. *Prostate*. 2014;74:702–13. <https://doi.org/10.1002/pros.22789>.
- Huang SS, DiFilippo F, Lindner D, Heston WD. Intriguing information from recent letter and article regarding unwanted targeting of salivary glands by PSMA ligands. *Eur J Nucl Med Mol Imaging*. 2023;50:2950–1. <https://doi.org/10.1007/s00259-023-06325-x>.

- Kalidindi TM, Lee SG, Jou K, Chakraborty G, Skafida M, Tagawa ST, et al. A simple strategy to reduce the salivary gland and kidney uptake of PSMA-targeting small molecule radiopharmaceuticals. *Eur J Nucl Med Mol Imaging*. 2021;48:2642–51. <https://doi.org/10.1007/s00259-020-05150-w>.
- Khreish F, Ebert N, Ries M, Maus S, Rosar F, Bohnenberger H, et al. (225)Ac-PSMA-617/(177)Lu-PSMA-617 tandem therapy of metastatic castration-resistant prostate cancer: pilot experience. *Eur J Nucl Med Mol Imaging*. 2020;47:721–8. <https://doi.org/10.1007/s00259-019-04612-0>.
- Kozikowski AP, Nan F, Conti P, Zhang J, Ramadan E, Bzdega T, et al. Design of remarkably simple, yet potent urea-based inhibitors of glutamate carboxypeptidase II (NAALADase). *J Med Chem*. 2001;44:298–301. <https://doi.org/10.1021/jm000406m>.
- Kozikowski AP, Zhang J, Nan F, Petukhov PA, Grajkowska E, Wroblewski JT, et al. Synthesis of urea-based inhibitors as active site probes of glutamate carboxypeptidase II: efficacy as analgesic agents. *J Med Chem*. 2004;47:1729–38. <https://doi.org/10.1021/jm0306226>.
- Kratochwil C, Giesel FL, Leotta K, Eder M, Hoppe-Tich T, Youssoufian H, et al. PMPA for nephroprotection in PSMA-targeted radionuclide therapy of prostate cancer. *J Nucl Med*. 2015;56:293–8. <https://doi.org/10.2967/jnumed.114.147181>.
- Kratochwil C, Bruchertseifer F, Giesel FL, Weis M, Verburg FA, Mottaghy F, et al. 225Ac-PSMA-617 for PSMA-targeted alpha-radiation therapy of metastatic castration-resistant prostate cancer. *J Nucl Med*. 2016;57:1941–4. <https://doi.org/10.2967/jnumed.116.178673>.
- Kratochwil C, Bruchertseifer F, Rathke H, Bronzel M, Apostolidis C, Weichert W, et al. Targeted alpha-therapy of metastatic castration-resistant prostate cancer with (225)Ac-PSMA-617: dosimetry estimate and empiric dose finding. *J Nucl Med*. 2017;58:1624–31. <https://doi.org/10.2967/jnumed.117.191395>.
- Kuo HT, Lin KS, Zhang Z, Zhang C, Merkens H, Tan R, et al. What a difference a methylene makes: replacing Glu with Asp or Aad in the Lys-urea-Glu pharmacophore of PSMA-targeting radioligands to reduce kidney and salivary gland uptake. *Theranostics*. 2022;12:6179–88. <https://doi.org/10.7150/thno.76571>.
- Laydner H, Huang SS, Heston WD, Autorino R, Wang X, Harsch KM, et al. Robotic real-time near infrared targeted fluorescence imaging in a murine model of prostate cancer: a feasibility study. *Urology*. 2013;81:451–6. <https://doi.org/10.1016/j.urology.2012.02.075>.
- Lee Z, Heston WD, Wang X, Basilion JP. GCP III is not the “off-target” for urea-based PSMA ligands. *Eur J Nucl Med Mol Imaging*. 2023;50:2944–6. <https://doi.org/10.1007/s00259-023-06265-6>.
- Lucaroni L, Georgiev T, Prodi E, Puglioli S, Pellegrino C, Favalli N, et al. Cross-reactivity to glutamate carboxypeptidase III causes undesired salivary gland and kidney uptake of PSMA-targeted small-molecule radionuclide therapeutics. *Eur J Nucl Med Mol Imaging*. 2023;50:957–61. <https://doi.org/10.1007/s00259-022-05982-8>.
- Mease RC, Kang CM, Kumar V, Banerjee SR, Minn I, Brummet M, et al. An improved (211)At-labeled agent for PSMA-targeted alpha-therapy. *J Nucl Med*. 2022;63:259–67. <https://doi.org/10.2967/jnumed.121.262098>.
- Mohan V, Bruin NM, Tesselar MET, de Boer JP, Vegt E, Hendriks J, et al. Muscarinic inhibition of salivary glands with glycopyrronium bromide does not reduce the uptake of PSMA-ligands or radioiodine. *EJNMMI Res*. 2021;1:25. <https://doi.org/10.1186/s13550-021-00770-1>.
- Rousseau E, Lau J, Kuo HT, Zhang Z, Merkens H, Hundal-Jabal N, et al. Monosodium glutamate reduces (68)Ga-PSMA-11 uptake in salivary glands and kidneys in a preclinical prostate cancer model. *J Nucl Med*. 2018;59:1865–8. <https://doi.org/10.2967/jnumed.118.215350>.
- Roy J, Warner BM, Basuli F, Zhang X, Wong K, Pranzatelli T, et al. Comparison of prostate-specific membrane antigen expression levels in human salivary glands to non-human primates and rodents. *Cancer Biother Radiopharm*. 2020;35:284–91. <https://doi.org/10.1089/cbr.2019.3079>.
- Roy J, Warner BM, Basuli F, Zhang X, Zheng C, Goldsmith C, et al. Competitive blocking of salivary gland [(18)F]DCFPyL uptake via localized, retrograde ductal injection of non-radioactive DCFPyL: a preclinical study. *EJNMMI Res*. 2021;1:66. <https://doi.org/10.1186/s13550-021-00803-9>.
- Sartor O, de Bono J, Chi KN, Fizazi K, Herrmann K, Rahbar K, et al. Lutetium-177-PSMA-617 for metastatic castration-resistant prostate cancer. *N Engl J Med*. 2021;385:1091–103. <https://doi.org/10.1056/NEJMoa2107322>.
- Schuchardt C, Zhang J, Kulkarni HR, Chen X, Muller D, Baum RP. Prostate-specific membrane antigen radioligand therapy using (177)Lu-PSMA I&T and (177)Lu-PSMA-617 in patients with metastatic castration-resistant prostate cancer: comparison of safety, biodistribution, and dosimetry. *J Nucl Med*. 2022;63:199–207. <https://doi.org/10.2967/jnumed.121.262713>.
- Siegel RL, Miller KD, Wagle NS, Jemal A. Cancer statistics, 2023. *CA Cancer J Clin*. 2023;73:17–48. <https://doi.org/10.3322/caac.21763>.
- Taieb D, Foletti JM, Bardies M, Rocchi P, Hicks RJ, Haberkorn U. PSMA-targeted radionuclide therapy and salivary gland toxicity: why does it matter? *J Nucl Med*. 2018;59:747–8. <https://doi.org/10.2967/jnumed.118.207993>.
- van Kalmthout LWM, Lam M, de Keizer B, Krijger GC, Ververs TFT, de Roos R, et al. Impact of external cooling with icepacks on (68)Ga-PSMA uptake in salivary glands. *EJNMMI Res*. 2018;8:56. <https://doi.org/10.1186/s13550-018-0408-2>.
- Wurzer A, Pollmann J, Schmidt A, Reich D, Wester HJ, Notni J. Molar activity of Ga-68 labeled PSMA inhibitor conjugates determines PET imaging results. *Mol Pharm*. 2018;15:4296–302. <https://doi.org/10.1021/acs.molpharmaceut.8b00602>.
- Yu H, Lv J, Hu P, Chen S, Shi H. Reduction of radiation accumulation in salivary glands through oral vitamin C during 68Ga-PSMA-11 total-body dynamic PET/CT imaging. *Nucl Med Commun*. 2022;43:166–71. <https://doi.org/10.1097/MNM.0000000000001506>.
- Zacherl MJ, Gildehaus FJ, Mittlmeier L, Boning G, Gosewisch A, Wenter V, et al. First clinical results for PSMA-targeted alpha-therapy using (225)Ac-PSMA-I&T in advanced-mCRPC patients. *J Nucl Med*. 2021;62:669–74. <https://doi.org/10.2967/jnumed.120.251017>.

Publisher's Note

Springer Nature remains neutral with regard to jurisdictional claims in published maps and institutional affiliations.